

## THE PHASING SYSTEM

H. A. Hogg, Editor, M. J. Lee, G. A. Loew,  
and A. R. Wilmunder

The function of the phasing system is to adjust the phases of the 245 klystrons so that the energy of the accelerated electron beam is maximized and the energy spectrum width is held to a minimum. To achieve this, the design objective of the automatic phasing system was to make the crests of the RF traveling wave in the accelerator coincide with the electron bunch centers within  $\pm 5^\circ$ . This objective has been met by the system described in this chapter.

During the initial design phase of the SLAC project, detailed studies were made of various proposals for phasing the machine.<sup>1-10</sup> Evaluation of these proposals, which are briefly reviewed here, led to the choice of the *beam induction* technique as the *modus operandi* for the automatic phasing system.

The drive system and the phasing system are covered in separate chapters of this book. However, a complete understanding of the automatic phasing system cannot be obtained without at least partial reference to the drive system described in Chapter 9. The reader who wishes to understand the basic motivations behind the design criteria imposed on the phasing system should at least read the introduction to that chapter. Hereinafter, the justifications for these criteria will be assumed. Hence, the discussion on phasing accuracy and the desire to maximize the energy of the accelerator to within 0.5% of its maximum value will not be repeated.

The energy spectrum width depends on phasing in the following way. If all accelerator sections are perfectly phased and the electrons are bunched with a uniform distribution within an angular spread  $\alpha$ , the energy spectrum width expressed as a fraction of maximum energy is

$$\frac{\Delta V_{\text{Tot}}}{V_{\text{Tot}}} = 1 - \cos \frac{\alpha}{2} \approx \frac{\alpha^2}{8} \quad (12-1)$$

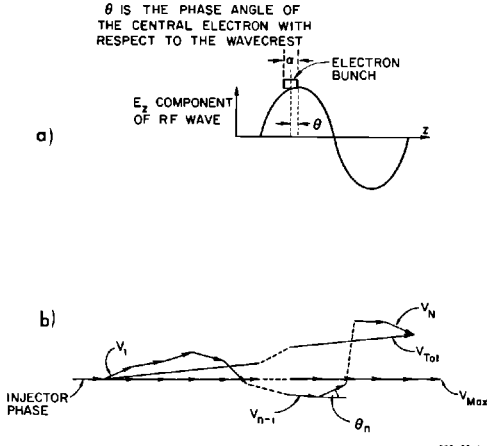


**Figure 12-1** Illustrating the effect of imperfect phasing.

However, if phasing is imperfect as shown in Fig. 12-1a, the fractional energy spread for small  $\alpha$  and  $\theta$  can be shown<sup>8</sup> to become

$$\frac{\Delta V_{Tot}}{V_{Tot}} \approx \frac{1}{2} \left[ \frac{\alpha}{2} + \frac{\sum \theta_n}{N} \right]^2 \quad (12-2)$$

where  $N$  is the number of sections and  $\sum \theta_n$  is the algebraic sum of the individual phasing errors. (See Fig. 12-1b.) Thus, the minimum obtainable energy spectrum width is determined by the bunching angle  $\alpha$ , but the energy spread is further degraded by the term  $\sum \theta_n/N$ . Fortunately, this term can experimentally be made equal to zero even if the individual values of  $\theta_n$  are not known. It is only necessary to adjust the phase of the injector klystron until the energy spectrum width out of the machine is minimized. This operation is commonly called “phase closure.” It is performed manually after the automatic phasing system has been operated.

Some alternative methods of phasing, either automatically or manually, will now be mentioned before proceeding to a detailed discussion of the adopted technique.

### 12-1 Survey of earlier phasing methods (GAL)

#### *Beam energy maximization*

With the exception of the 2-GeV Kharkov Linear Accelerator in the U.S.S.R., no linear electron accelerator built or conceived before the SLAC machine ever required an automatic phasing system. In multisection accelerators, the practice so far has been to optimize the phase of each klystron individually

by maximizing energy output and minimizing spectrum width. This corresponds to setting all  $\theta_n$  equal to zero in Fig. 12-1b, so that  $V_{\text{Tot}}$  coincides with  $V_{\text{Max}}$ . The method, known as "beam energy maximization," has the disadvantage that its sensitivity is inversely proportional to the number of klystrons in operation. A change in phase of  $\pm 5^\circ$  about the optimum for 1 klystron in 240 gives a fractional energy change of 0.0016%. From this it is clear that beam energy maximization is not a very good way of phasing a long machine. The sensitivity can be improved by observing the current in part of the electron beam after dispersion by a momentum spectrometer. The change in current in a certain energy width is observed as the RF phase is rotated. However, this method, which is known as the "current variation detection (CVD) technique,"<sup>1,6,7</sup> is also insufficiently sensitive and interferes with the beam available for physics experiments. In addition, both methods are slow and require the establishment of a beam through the entire machine prior to phasing—a condition which is probably impossible to fulfill.

#### *Direct phase comparison*

A method based on direct phase comparison between adjacent RF feed lines just before they connect to the accelerator was considered. It is apparent that, in order to be sure that the waves in successive accelerator sections are correctly phased within the allowed tolerance, the electrical lengths of all RF lines involved must be known very precisely, not only at the time of installation, but subsequently when the temperature has changed and building movements may have occurred. In any case, such a direct comparison ensures only that all the RF waves are correctly phased with respect to each other but not necessarily with respect to the beam. The later phase alignment has to be achieved by another method, such as the CVD technique mentioned above. (It should be remembered that the CVD technique has a workable sensitivity when it is applied to whole sectors of the machine instead of individual klystrons.)

#### *Interaction between electron beam and RF wave*

Two further methods of phasing were proposed. These depend upon measurement of changes in resistive and reactive beam loading as the relative phases of beam and RF wave are changed in an accelerator section.

When an electron beam passes through an accelerator section filled with RF energy, a fraction of this energy is delivered to the beam, and the RF power at the output of the section decreases. This effect is known as *resistive beam loading*. The section is correctly phased when the power reduction is a maximum. If a phase error  $\theta$  exists between the electron bunches and the wave, the steady-state RF power flow at the exit of a constant gradient accelerator section is

$$P = P_0 e^{-2\tau} + rLi^2 \left[ \frac{\tau^2}{e^{2\tau} - 1} \right] - 2i \left[ P_0 rL \left( \frac{\tau^2}{e^{2\tau} - 1} \right) e^{-2\tau} \right]^{1/2} \cos \theta \quad (12-3)$$

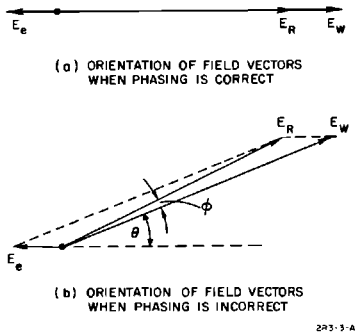


**Figure 12-2** Vector diagram illustrating principle of phasing accelerator section by reactive beam-loading method.

where  $P_0$  is the RF input power, and all other symbols have been defined in Chapter 6. Unfortunately, the cosine term makes the effect a poor criterion for correctness of phasing, since  $dP/d\theta$  is proportional to  $\sin \theta$ . Thus the sensitivity tends to zero as the optimum phase relationship is approached.

*Reactive beam loading* may be understood by referring to Fig. 12-2. Here  $\mathbf{E}_W$  is the electric field vector of the impressed RF wave from the klystron power source. The magnitude of  $\mathbf{E}_W$  is approximately constant along a constant gradient accelerator section. The beam induces a wave of which the electric field vector is represented by  $\mathbf{E}_e$ . The magnitude of this vector grows with distance as<sup>11</sup>

$$E_e = \frac{ir}{2} \ln \left[ 1 - \left( \frac{z}{L} \right) (1 - e^{-2\tau}) \right] \quad (12-4)$$

where again, the symbols are defined in Chapter 6.  $\mathbf{E}_R$  is the vector sum of  $\mathbf{E}_W$  and  $\mathbf{E}_e$ , and its magnitude is given by

$$E_R^2 = E_e^2 + E_W^2 - 2E_e E_W \cos \theta \quad (12-5)$$

Figures 12-2a and b show the vector orientations for correct and incorrect phasing, respectively.  $\phi$  is the phase angle between  $E_R$  (beam on) and  $E_W$  (beam off). It is the quantity which has to be measured and adjusted to zero in this method of phasing. It may be seen that

$$\lim_{\theta \rightarrow 0} \left| \frac{d\phi}{d\theta} \right| = \frac{1}{E_W/E_e - 1} \quad (12-6)$$

The ratio  $E_W/E_e$  at the end of a 10-ft accelerator section fed by a 24-MW klystron, with 1 mA of accelerated beam current is approximately 500. Therefore the sensitivity of this method of phasing is also low.

### 12-2 Theory of beam induction technique (HAH, MJL)

Examination of the reactive beam loading method of phasing, which involves an indirect measurement of the phase of the beam-induced wave in an accelerator section, led to the *beam induction* method which was chosen for the two-mile machine.

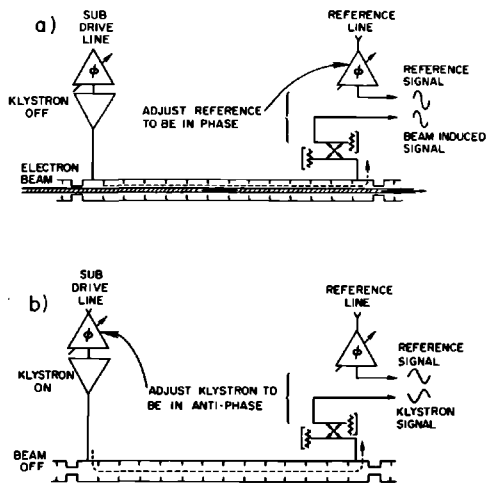
The principle of the beam induction technique is as follows:

1. With the klystron wave turned off, the phase of the beam-induced wave in the particular accelerator section to be phased is compared with a coherent cw reference signal of the same frequency.
2. The phase of the reference signal is adjusted to be the same as the phase of the beam-induced signal at the place where the comparison is made. See Fig. 12-3a.
3. The phase of the reference signal is then locked.
4. The klystron is turned on, and the phase of the klystron wave in the accelerator section is compared with the reference signal.
5. The phase of the klystron signal is adjusted to be  $180^\circ$  away from the phase of the reference signal. (See Fig. 12-3b.)

For the reasons explained above and illustrated in Figs. 12-1 and 12-2, the klystron is then optimally phased.

Actually, for clarity in the statement of the principle of operation, one oversimplification of the system was made which requires correction: when the phase comparison between beam-induced and reference signals is being

**Figure 12-3** Illustrating beam-induction method of phasing accelerator.



made, there is no need to turn the klystron off. Indeed, to do so is undesirable because removal of RF power from an accelerator section allows it to cool down, with a consequent change in its dimensions and propagation characteristics. Since the accelerator is a pulsed machine, it is only necessary to delay the klystron pulse by a suitable interval, typically 50  $\mu$ sec, during the phasing operation instead of turning it off.

The delayed position of the klystron pulse with respect to the beam pulse is referred to as the "standby" position.

The beam-induction method has a number of advantages but also poses certain problems that will be discussed below. The advantages are

1. It has the best sensitivity of all the methods which were studied. Since  $\theta$  is measured directly,

$$\frac{\text{sensitivity (beam induction method)}}{\text{sensitivity (reactive beam loading method)}} = \lim_{\theta \rightarrow 0} \left( \frac{1}{|d\phi/d\theta|} \right) = \frac{E_w}{E_e} \quad (12-7)$$

As mentioned above this ratio can be as large as 500 : 1.

2. The beam-induced and klystron signals are sampled directly at the accelerator and are transmitted along a common cable to the phase detection circuit in the klystron gallery. The phase comparison is, therefore, essentially direct; the length of the cable does not need to be known, and the attainable sensitivity and accuracy are good.
3. There need be very little interference with physics experiments, because only one klystron at a time need be "set to standby" as the phasing operation progresses along the machine.
4. Klystrons which are placed on "standby" for reasons other than phasing can be maintained correctly phased with respect to the beam so that they are instantly available for acceleration, on demand.

Among the problems, the most serious relates to the very large difference between the power levels of the beam-induced and the klystron signals. The extremes of the specified conditions under which the phasing system will be required to operate have to be considered, viz., a beam current pulse as low as 1 mA and a klystron peak power input to one 10 ft accelerator section as high as 24 MW. The attenuation per 10-ft section is approximately 5 dB and the beam-induced power at the output of the section is 26 W/(mA)<sup>2</sup>, so that the largest power ratio of the two signals at the end of the 10-ft section is roughly 54 dB.

Well-known devices such as the slotted line, "magic T," and hybrid ring are normally used for the phase comparison of two signals. A minimum or a null in the detected output from one arm of these devices indicates a given phase relationship between the two signals. A null is obtained only if the two signals are of equal amplitude. As the difference between the amplitudes of

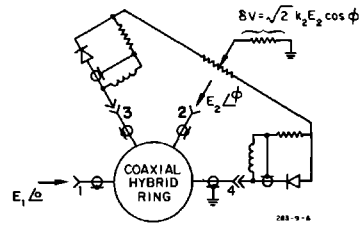


Figure 12-4 Hybrid ring phase comparator.

the two signals increases, the phase-indicating null is replaced by a broad minimum, and the balance point becomes increasingly difficult to detect. The method is unreliable when the signals differ by more than 10 dB. Moreover, the *overall* phase detection system that is required is one which will develop an error signal depending only upon the phase difference between the two input signals. Considering that the phase comparison network is just a *part* of the overall system, it will be shown later that its error signal can be permitted to vary by not more than 4 to 1 over the entire range of input signal levels.

The performance of a perfect hybrid ring used as a phase comparison network will now be examined (Fig. 12-4). The signals to be compared are applied to arms 1 and 2, and arms 3 and 4 are terminated in matched detectors. Let the electric field amplitudes of the input signals be  $E_1$  and  $E_2$ . Then the outputs to the detectors are given by

$$E_3^2 = \frac{E_1^2}{2} + \frac{E_2^2}{2} + E_1 E_2 \cos \phi \quad (12-8)$$

and

$$E_4^2 = \frac{E_1^2}{2} + \frac{E_2^2}{2} - E_1 E_2 \cos \phi \quad (12-9)$$

where  $\phi$  is the phase difference between  $E_1$  and  $E_2$  at arms 1 and 2.

Let  $E_2$  represent the reference signal and  $E_1$  either the beam-induced or the klystron signal, and let  $E_1 \geq E_2$ .

If the detectors have an index  $n$ , their responses are

$$V_3 = kE_3^n \quad (12-10)$$

and

$$V_4 = kE_4^n \quad (12-11)$$

where  $k$  is a constant.

It follows that the difference between the detected signals is given by

$$\delta V = \frac{k}{2^{n/2}} [(E_1^2 + E_2^2 + 2E_1E_2 \cos \phi)^{n/2} - (E_1^2 + E_2^2 - 2E_1E_2 \cos \phi)^{n/2}] \quad (12-12)$$

so that

$$\delta V_{\max} = \frac{k}{2^{n/2}} [(E_1 + E_2)^n - (E_1 - E_2)^n] \quad (12-13)$$

Two cases are of special interest. If the detectors are "square-law" ( $n = 2$ ),

$$\delta V = 2k_1 E_1 E_2 \cos \phi \quad (12-14)$$

where  $k$  has been set equal to  $k_1$ . Then

$$\delta V_{\max} = 2k_1 E_1 E_2 \quad (12-15)$$

Thus, for square-law detectors, the differential output voltage  $\delta V$  for a given phase error is proportional to both  $E_1$  and  $E_2$ . The reference  $E_2$  can be constant, but  $E_1^2$  is variable over a 54-dB range; therefore, square-law detectors are quite unsuitable for use in the phasing system.

On the other hand, if the detectors are linear,  $n = 1$  and Eq. (12-13) becomes

$$\delta V_{\max} = \sqrt{2} k_2 E_2 \quad (12-16)$$

where  $k$  has been set equal to  $k_2$ .

When  $n = 1$  and  $E_1 \gg E_2$ , Eq. (12-12) becomes

$$\delta V = \sqrt{2} k_2 E_2 \cos \phi \quad (12-17)$$

and the sensitivity,  $\partial(\delta V)/\partial\phi$ , is  $-\sqrt{2} k_2 E_2$  at  $\delta V = 0$ .

When  $n = 1$  and  $E_1 = E_2$ , Eq. (12-12) becomes

$$\delta V = \frac{1}{\sqrt{2}} \sqrt{2} k_2 E_2 \left( \cos \frac{\phi}{2} - \sin \frac{\phi}{2} \right) \quad (12-18)$$

and the sensitivity at  $\delta V = 0$  is  $-k_2 E_2$ .

In Fig. 12-5,  $\delta V$  is plotted as a function of  $\phi$  for both cases. It is seen that the use of linear detectors removes the  $\delta V$  dependence on  $E_1$ , so that with constant  $E_2$ ,  $\delta V$  is a function of  $\phi$  only. As  $E_1$  decreases from very large values to equality with  $E_2$ , the sensitivity of null detection decreases by a factor of only  $1/\sqrt{2}$ .

It should be mentioned now that no detector will remain perfectly linear over the specified range of input powers. The best approximation presently available is a coaxial thermionic diode, which maintains an index of less than 1.2 over the required range.

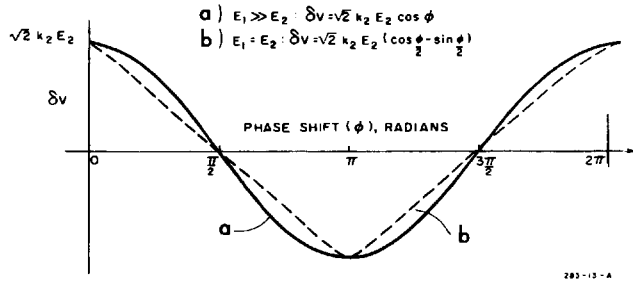


Figure 12-5 Plot of  $\delta V$  vs  $\phi$  for linear diodes.

The effect of diode nonlinearity may be estimated as follows. Let the range of  $E_1$  be  $E_b \leq E_1 \leq E_a$ , and let  $E_b = mE_2$ , where  $m \geq 1$ . Assume that the diode index  $n$  changes from  $1 + \epsilon$  to 1 as  $E_1$  changes from  $E_b$  to  $E_a$ . The ratio  $R$  of  $(\delta V)_{\max}$  at the extremes of the range of  $E_1$  is given by

$$R = \frac{(\delta V)_{\max} |_{n=1, E_1=E_a}}{(\delta V)_{\max} |_{n=1+\epsilon, E_1=E_b}} < R_{\max}$$

where

$$R_{\max} = \frac{(\delta V)_{\max} |_{n=1+\epsilon, E_1=E_a}}{(\delta V)_{\max} |_{n=1+\epsilon, E_1=E_b}}$$

Substituting from Eq. (12-13) and expanding the numerator gives

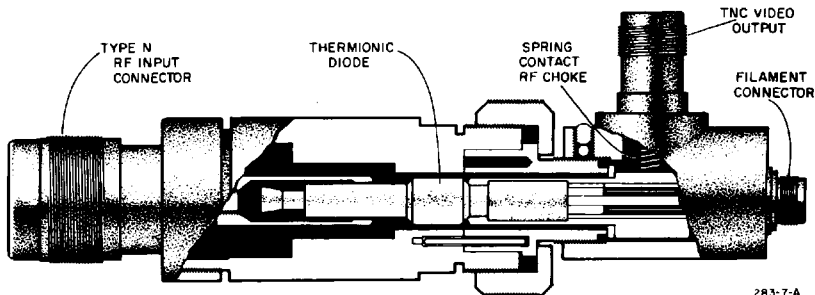
$$R_{\max} = \frac{2(1 + \epsilon)(mE_a/E_b)^\epsilon}{(m + 1)^{1+\epsilon} - (m - 1)^{1+\epsilon}} \tag{12-19}$$

which becomes  $(E_a/E_b)^\epsilon$  for large  $m$ . The extreme operating conditions are  $m = 1$  and  $(E_a/E_b)^2 = 54$  dB. When  $\epsilon = 0.2$ , these conditions give  $R_{\max} \approx 3.4$ .

From this, it will be seen that the coaxial thermionic diode is acceptable.

The detector used is an RCA Type 6173 coaxial thermionic diode mounted in a special housing designed at SLAC (see Fig. 12-6). The anode is held in

Figure 12-6 Thermionic diode and housing.



position by spring fingers and connected to the center conductor of the Type N input RF connector. The detected output is taken from the cathode to a TNC connector on the side of the diode housing. The filament power is supplied through a separate twin-axial connector.

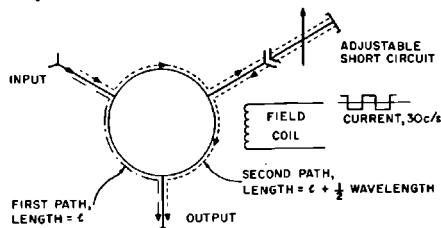
The diode resistive loads are connected in opposition by a balancing potentiometer, the wiper of which may be adjusted to offset asymmetries in the hybrid ring, diodes, and diode loads. In theory, the differential diode output as described contains the required phase information. If the diodes are balanced, then as the phase angle  $\phi$  rotates, the differential output will oscillate about zero, passing through zero when  $\phi = (p \pm \frac{1}{2})\pi$ , where  $p$  is an integer. The direction from which zero is approached with increasing  $\phi$  may be used to avoid  $\pi$  ambiguity in phase setting (see Fig. 12-5). However, such a system is impracticable because it depends on dc balancing. The long-term stability required of the diodes and the following dc amplifiers would be very difficult to achieve. This difficulty constitutes the second serious problem in the development of the beam-induction phasing system. The problem is avoided by the use of a technique which has become known as "phase wobbling."

### 12-3 The principle of "phase wobbling" (HAH, MJL)

The dc phase-detection system described above is converted to an ac system by phase-modulating the reference signal,  $E_2$ . This artifice immediately removes most of the problems of drift in dc levels and provides a method of instructing the automatic servo system whether the phase of  $E_1$  is leading or lagging the phase of the reference,  $E_2$ .

Phase wobbling is achieved by the use of a three-port switching circulator in the reference line (see Figs. 12-7 and 12-8). The reference signal enters through one port and propagates to the output port either directly or through a third port, depending upon the polarity of the field used to magnetize the ferrite material. The third port is terminated by an adjustable short circuit, so that the difference between the two path lengths to the output port can be made one-half wavelength. The direction of current flow in the magnetizing coil is reversed before the arrival of each successive beam-induced or klystron

Figure 12-7 Switching circulator used as phase wobbler.



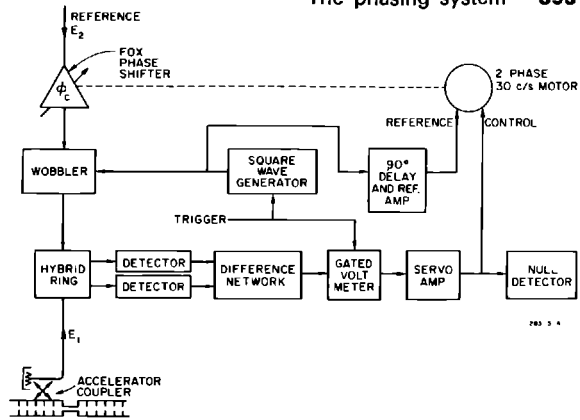


Figure 12-8 Block diagram of phase-wobbling system.

RF pulse. Hence the cw reference signal,  $E_2$ , is square-wave, phase-modulated at 30 Hz so that successive beam-induced or klystron pulses are compared with reference signals which differ in phase by  $\pi$ .

The principle of the phase wobbling technique is essential to the automatic phasing system which has been developed, so that a description of the former introduces the main features of the latter.

A block diagram of the system is shown in Fig. 12-8. The cw reference signal  $E_2$  is transmitted to the wobbler through a "Fox"-type rotary phase shifter,<sup>12</sup>  $\phi_c$ . This design of phase shifter was chosen because the phase shift it introduces is a linear monotonically increasing function of the angle of rotation of the phase-shifter drum. There are no discontinuities or end stops. The wobbler is driven by a 30-Hz square-wave generator, synchronized by a 60-pulses/sec trigger. The wobbler output is connected to the hybrid ring, where the accelerator signal  $E_1$  interacts with reference  $E_2$  as described above. The output ports are terminated by the two thermionic diode detectors, and the differential output is fed into a gated voltmeter.

To understand the operation of the system so far described, the reader is referred to Figs. 12-8 and 12-9. Let the drum of the Fox phase shifter be slowly rotated so that the phase difference  $\phi$  between  $E_1$  and  $E_2$  at the hybrid ring increases from 0 to  $2\pi$  in a time  $2T_p$ , where  $2T_p$  is a few seconds. See Figs. 12-9a and b. The wobbler is phase-modulating  $E_2$  by  $\pm\pi/2$  at 30 Hz, so that the phase of  $E_2$  at the hybrid ring changes by  $\pi$  every 1/60 sec. Pulses of signal  $E_1$  are arriving from the accelerator at the rate of 60 per second, the pulse length being 1–2.5  $\mu\text{sec}$ . The trigger for the wobbler driver assures that  $E_2$  changes phase in the interval between the arrival of  $E_1$  pulses.

It was shown above that the balanced differential output from two linear diodes is  $\sqrt{2}k_2 E_2 \cos \phi$ . It follows that, as  $E_2$  is wobbled, the differential output pulse amplitudes will change from  $\sqrt{2}k_2 E_2 \cos[\phi + (\pi/2)]$

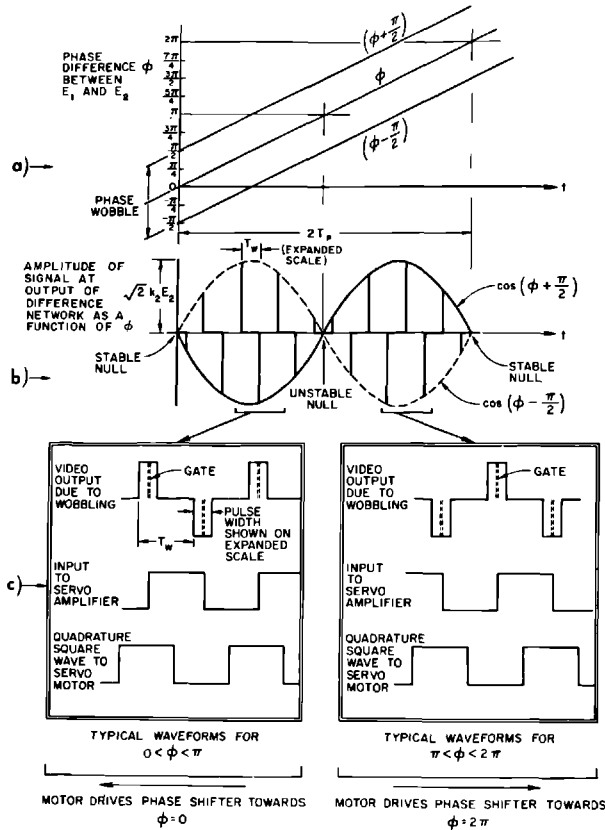


Figure 12-9 Illustrating the application of phase wobbling to an automatic phasing system.

to  $\sqrt{2} k_2 E_2 \cos[\phi - (\pi/2)]$  in a time  $T_w = 1/60$  sec. (For clarity, the "wobbled" time scale in Fig. 12-9b has been expanded.)

To see what happens next, the output pulses are further expanded in the top line of Fig. 12-9c. To avoid beginning and end-of-pulse transients, the pulse amplitudes are sampled by a "gate,"  $0.2 \mu\text{sec}$  wide, located near the center of the pulse. The sample is held until the next pulse arrives, so that a 30-Hz square wave is formed with amplitude proportional to  $\cos[\phi + (\pi/2)]$ . This wave is amplified and fed to the control winding of a two-phase motor which drives  $\phi_c$ .

Going back to the wobbler driver (square-wave generator in Fig. 12-8), part of the square-wave output is fed to a  $90^\circ$  delay circuit followed by an amplifier stage, giving a constant amplitude square-wave output which is in quadrature with the wobbler drive signal. This signal energizes the reference winding of the two-phase motor. The motor will develop a torque proportional to the product of the amplitudes of the applied square waves. The

direction of rotation will depend upon whether the control wave leads or lags the reference wave.

From Figs. 12-9a and b, when  $0 < \phi < \pi$ ,

$$E_2 \cos\left(\phi + \frac{\pi}{2}\right) < 0 < E_2 \cos\left(\phi - \frac{\pi}{2}\right) \quad (12-20)$$

Therefore the motor is connected so that, under these conditions, the phase shifter rotates towards  $\phi = 0$ .

It follows that when  $\pi < \phi < 2\pi$ ,

$$E_2 \cos\left(\phi + \frac{\pi}{2}\right) > 0 > E_2 \cos\left(\phi - \frac{\pi}{2}\right) \quad (12-21)$$

and the phase shifter rotates toward  $\phi = 2\pi$ , which is identical with  $\phi = 0$ .

The system thus connected always drives  $\phi_c$  away from the unstable null at  $\phi = \pi$  toward the stable null at  $\phi = 0$ . It should be noted that an identically connected phase shifter in the *other* input arm to the hybrid ring will rotate toward a stable null at  $\phi = \pi$ .

Before proceeding to a description of the complete automatic phasing system, two further comments on the wobbler technique will be made.

First, it is easy to show that errors which would otherwise be introduced by differing diode conversion efficiencies are eliminated by phase wobbling. This is an important advantage, because it is not possible to obtain a perfectly matched pair over the entire range of signal levels.

Let the output voltages of the two diodes be

$$V_3 = k_3 E_3^n$$

and

$$V_4 = k_4 E_4^n$$

For the two wobbler positions ( $\pm \pi/2$ ) the difference between the output voltages is given by Eq. (12-12)

$$\begin{aligned} \delta V|_{(\phi \pm \pi/2)} &= \frac{k_3}{2^{n/2}} \left[ E_1^2 + E_2^2 + 2E_1 E_2 \cos\left(\phi \pm \frac{\pi}{2}\right) \right]^{n/2} \\ &\quad - \frac{k_4}{2^{n/2}} \left[ E_1^2 + E_2^2 - 2E_1 E_2 \cos\left(\phi \pm \frac{\pi}{2}\right) \right]^{n/2} \quad (12-22) \end{aligned}$$

The automatic system indicates a phase balance when the difference between the detected outputs in the two wobbler positions is zero, i.e.,

$$\delta V|_{(\phi + \pi/2)} = \delta V|_{(\phi - \pi/2)}$$

This occurs when  $\phi = 0 \pm p\pi$ , independently of the values of  $k_3$  and  $k_4$ .

The second point to be made is that imperfections in the switching circulator do not affect phasing accuracy. It can be shown<sup>13</sup> that if the phase difference introduced by switching from one path to the other is not exactly  $\pi$ , or if the two paths have different insertion losses, no phase error is introduced.

## 12-4 Functional description of the system (HAH, ARW)

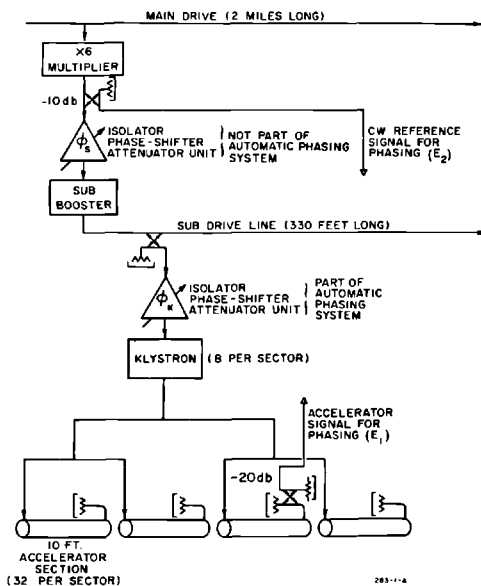
### *Sector phasing equipment*

As for most other systems, a sector was chosen as the subdivision of the machine for the purpose of phasing. This division is convenient since all the necessary status signals concerning the modulators and klystrons are available at the "instrumentation and control" alcove located approximately in the middle of a sector. It also reduces the length of the control wires and RF cables, thereby reducing attenuation and phase drift.

Figure 12-10 is a schematic of the RF drive system in one sector. The 476-MHz main drive signal is multiplied to 2856 MHz, at which point  $-10$  dB of the power is coupled off to provide the reference signal,  $E_2$ , for the phasing system. The remainder of the signal is used to drive the sub-booster amplifier, which feeds 360 pulse-pairs/sec into the subdrive line.

As described in Chapter 9, power is coupled from the subdrive line at eight points, each coupler feeding one 24-MW klystron through an isolator, phase-shifter, attenuator unit. The phase shifter in this unit is of the type already described. It is coupled to the automatic phasing system and will be referred to as the "klystron phase shifter,"  $\phi_k$ . The RF output from each klystron feeds four 10-ft accelerator sections, as shown. As discussed in

**Figure 12-10** Drive system schematic for one module of the machine, showing how the signals for the phasing system are derived.





is a special switching unit which ensures that the steps described in the previous section are carried out in sequence, and repeated "down the line" until all eight klystrons in one sector are properly phased.

### Basic operation

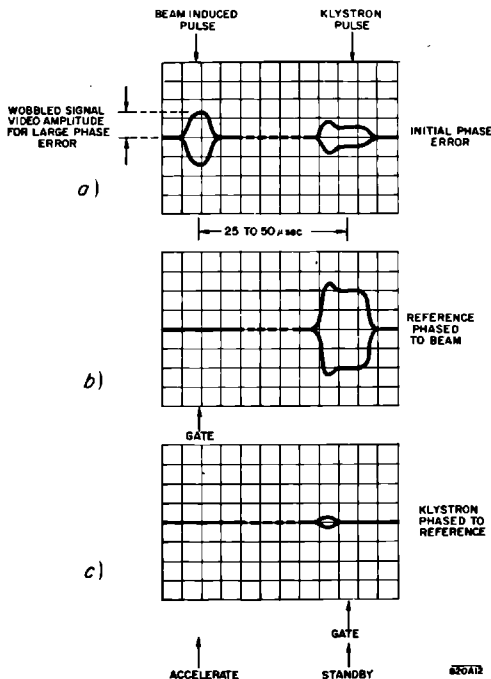
The operation of the complete system is as follows:

1. When the programmer is activated by pressing either the local or Central Control Room (CCR) "start" button, klystron No. 1 is set to the "standby" pulse position. Switches in the RF detector panel connect the appropriate accelerator section output to the hybrid ring, and the phase of the beam-induced wave is compared with the reference signal. A typical CRO trace of the video signal at the output of the diode network before phasing is shown in Fig. 12-12a.

2. The control phase shifter,  $\phi_c$ , rotates towards a stable null until the servo amplifier output drops below 4 V. The motor then stops and the null detector indicates that the programmer may advance to the "klystron-phase" position. [See the CRO trace in Fig. 12-12b.]

3. A brake is applied to  $\phi_c$ .

**Figure 12-12** RF detector panel video output traces at three stages of phasing.



4. Provided that klystron No. 1 is operating properly, the “gate” of the gated voltmeter shifts to sample the standby klystron pulse, so that the phase of the klystron wave is compared with the reference.

5. The klystron phase shifter,  $\phi_k$ , preceding klystron No. 1 is connected to the electronics panel by the programmer and rotates to a stable null which is  $\pi$  away from the stable null of  $\phi_c$  because it is in the other signal input arm to the hybrid ring. A typical CRO trace of the video signal at the output of the diode network after phasing is shown in Fig. 12-12c.

6. When the null detector indicates that the phasing error is within the accepted tolerance, the programmer switches to klystron No. 2, setting it to standby and returning No. 1 to accelerate. The phasing cycle is then repeated.

7. The phasing operation continues until all eight klystrons are phased.

8. When the null detector indicates that the last klystron in the sector has been phased, the programmer energizes switches in the RF detector panel, connecting a sample signal from the sector subdrive line to  $\phi_c$ . At the same time, the other input arm of the hybrid ring is switched to the output of a reference cavity located in the drift section at the end of the previous sector (shown schematically in Fig. 12-11). This reference cavity is a re-entrant cavity resonant at 2856 MHz, the axis of which is collinear with the accelerator axis, so that the bunched beam passes through it. Part of the beam-induced output signal from the cavity is used as a normalizing signal for the beam position monitoring system, and part is used to provide a sector phase reference signal. (For more details, see Chapter 25.)

9. The phases of the cavity and subdrive line signals are compared at the hybrid ring, and the automatic servo system rotates  $\phi_c$  until a stable null is reached with the servo amplifier output voltage below 4 V. At this point, the brake is applied to lock the position of  $\phi_c$  and the programmer switches itself off. However, the electronics and RF detector panel are not de-energized so that the phase balance between the cavity and subdrive line signals continues to be monitored. If a phase drift occurs such that the servo amplifier output voltage exceeds 4 V, a warning light appears in the sector instrumentation alcove and in the central control display. The phase drift may be corrected either by automatically rephasing the sector or by rotating the phase shifter preceding the sub-booster (Fig. 12-10).

### *Special features*

The simple logic enumerated above is complicated by the following features:

1. Signals are received at the programmer from each modulator/klystron control unit (see Chapter 15) indicating whether the modulator is on or off and whether there is an RF output from the klystron. If both “no modulator” and “no RF” signals are received, no phase adjustments are attempted, and the programmer steps on to the next klystron. If, however, the indication is

that the modulator is available but there is no RF output, the programmer waits for recycling of the modulator to be completed. When RF again appears, it is phased. If the modulator goes off, the programmer steps to the next klystron.

2. If the "no RF" indication persists, or the phasing system fails to reach a null for any reason, the programmer may be stepped to the next klystron by pressing the "fault override" button (again, either on the programmer panel or in CCR).

3. The programmer may be made to step through without setting klystrons to standby or phasing by pressing a "don't phase" button in CCR, or holding down the "fault override" on the programmer panel.

4. The programmer may be stopped at any position by pressing a "stop" button in CCR or pressing and holding the "start" button on the programmer panel.

5. The programmer stops if the video output of one coaxial thermionic diode detector falls below a preset level (corresponding to a 1-mA peak beam current) or if the beam pulse repetition rate in the first time slot is lower than 60 pulses/sec.

6. Any phase shifter in one sector may be rotated locally by means of a manually controlled power supply built into the programmer.

### *Special phasing systems*

1. In sectors containing more than eight klystrons, subprogrammer units are used to quadruple the capacity of the main programmer. This means that at a future date the phasing system can be expanded to handle up to thirty-two klystrons per sector. At present, subprogrammers are used only in Sectors 1 and 11, where extra klystrons are required for initial acceleration of electron and positron beams, respectively.

2. When the "standby" injector klystron is brought on line, it is necessary to ensure that it has the same phase as the one it replaces. This is achieved by the system shown in Fig. 12-13. A special RF detector panel compares the phase of the subdrive-line signal (after the injector phase shifter) with the phase of the high-power signal in the common waveguide output. The differential video output is fed to a standard phasing electronics panel which generates the reference and control servo waveforms. These are routed to the  $I\phi A$  unit in the drive to the "on-line" klystron. A control panel in the injector alcove allows the  $I\phi A$  unit to rotate the klystron phase until the electronics panel indicates a null, then removes the control signal and applies the phase-shifter brake. When the klystron changeover switch is actuated, servo control is momentarily applied to the other  $I\phi A$  unit, so that the original phase relationship at the RF detector panel is restored. The overall injector phase is controlled by the injector phase shifter.

3. In addition to the standard two-phase ac motor in the phasing servo system, the  $I\phi A$  units in Sector 27 can be driven by stepper motors controlled

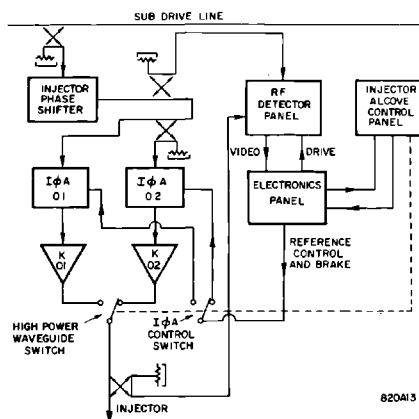


**Figure 12-13** Automatic injector klystron phase control.

from CCR. When required, these motors are coupled to the Fox phase-shifter drums by electromagnetic clutches. The system allows fine phase control for vernier energy adjustments to multiple beams.

## 12-5 Description of main and auxiliary components (HAH, ARW)

### *Cables for transmission of phasing signals*

In order to transmit the RF signals from the accelerator to the RF detector panel with the minimum of loss and yet with some flexibility in installation,  $\frac{7}{8}$ -in. coaxial cables are used. The 50-ohm cable has an attenuation of 2.8 dB/100 ft and a peak power handling capacity of over 60 kW.

The variation in phase shift through the cable due to ionizing radiation has been calculated and has been shown to be negligible for the radiation levels in the accelerator housing and for the lengths of cable which are exposed.

### *The IφA units*

As already mentioned in Chapter 9, *IφA* is a convenient abbreviation for isolator, phase shifter, attenuator. A typical unit is shown in Fig. 9-11. The input is connected by a  $\frac{1}{2}$ -in. semirigid coaxial cable to a subdrive-line coupler. The RF signal (360 pulse-pairs/sec, pulse width 2.5  $\mu$ sec, 4-kW peak power) travels through the phase shifter, which is protected from mismatches by two coaxial isolators. The signal is then coupled into the strip-line dual attenuator

assembly through a flexible cable whose phase shift-versus-temperature characteristic is of opposite sign to the rest of the unit. The cable length is chosen to keep the phase shift below  $0.1^\circ/\text{F}$  in the range of  $70^\circ$  to  $130^\circ\text{F}$ . The function of the manual and protection attenuators is described in Chapter 9. Before the output is connected to the main klystron, there is a dual directional coupler for monitoring forward and reflected power.

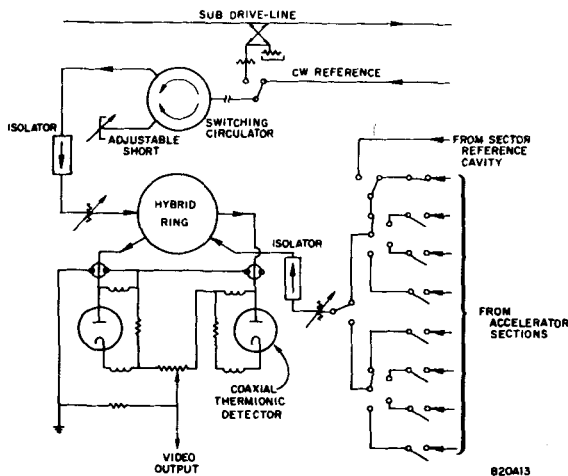
### *The control phase shifter*

A control phase-shifter unit consists of a Fox phase shifter, identical to the  $I\phi A$  phase shifter, mounted on a smaller chassis. Isolators are provided on the input and output.

### *The RF detector panels*

A simplified schematic of the microwave circuit in an RF detector panel is shown in Fig. 12-14. The wobbler and phase detection components have already been described. The nine-position selector switch is actually made up as a tree of coaxial switches. This arrangement has the advantages that it can be constructed from readily available commercial switches and gives an interchannel cross-talk isolation of about 100 dB, which is in excess of this system's requirements. The RF switches are operated either automatically by the programmer or manually by a control switch on the front of the panel. Provision is also made for monitoring various RF and video signals. A completed unit is shown in Fig. 12-15.

**Figure 12-14** Simplified schematic diagram of RF detector panel.



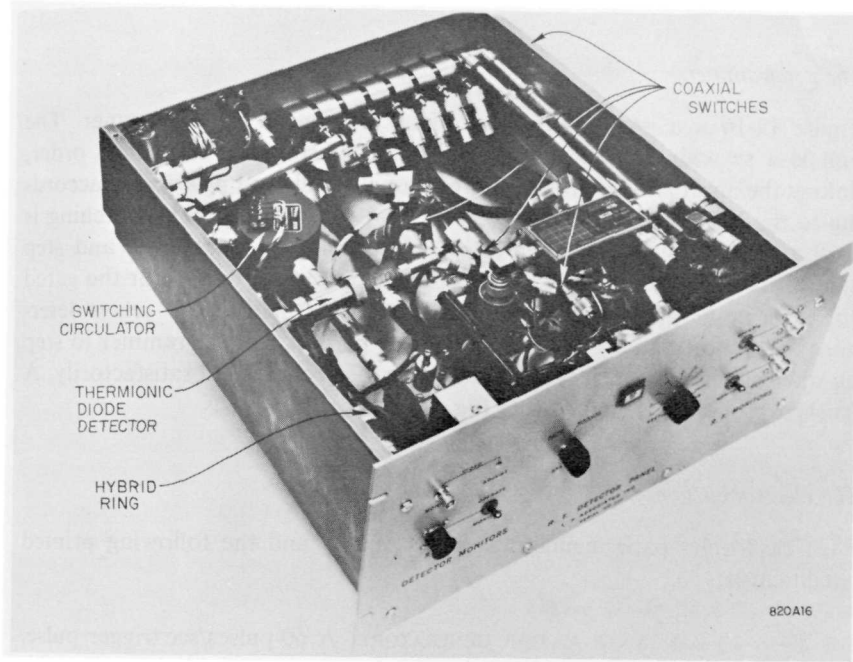
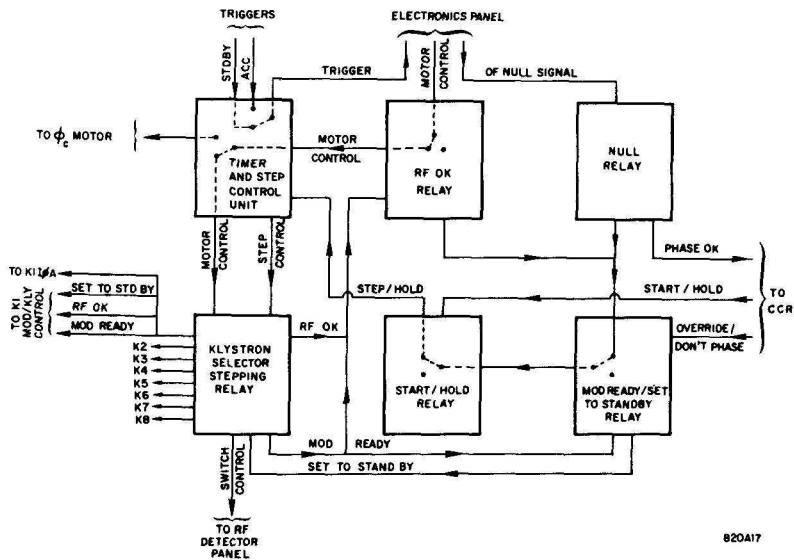


Figure 12-15 An RF detector panel.

Figure 12-16 Block diagram of phasing programmer.



### *The programmers*

Figure 12-16 is a greatly simplified block diagram of a programmer. The unit is a switching system which selects the klystrons in numerical order, linking the appropriate control and readout channels and proceeding according to the logic described under Section 12-4. Station-to-station switching is performed by a single stepping relay, which is driven by a timer and step control unit. The latter unit also selects the appropriate trigger for the gated voltmeter in the electronics panel. "RF OK" and "mod ready" relays determine the station status, and the "null" relay permits the programmer to step on when a particular phasing operation has been completed satisfactorily. A finished programmer is shown in Fig. 12-17.

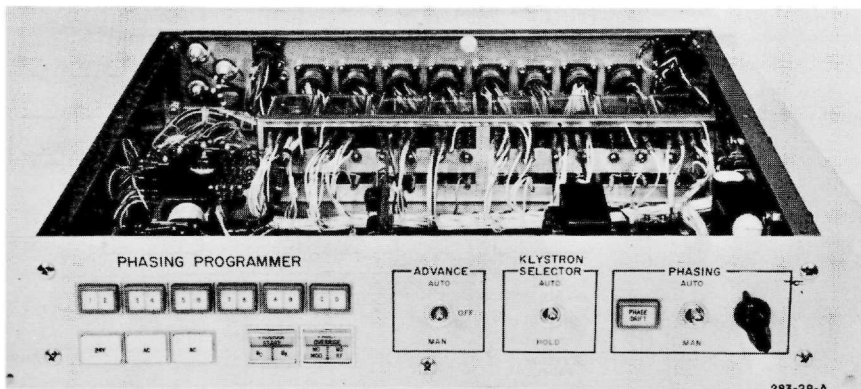
### *The electronics panels*

Each electronics panel contains a power supply and the following printed circuit cards:

THE 30-Hz SQUARE WAVE MASTER GENERATOR. A 60-pulses/sec trigger pulse, selected by the programmer, is used to trigger a master divide-by-two multivibrator. The output of this multivibrator drives an amplifier to provide power to operate the phase wobbler and the 90° delay and servo reference amplifier.

THE 90° DELAY AND REFERENCE AMPLIFIER. The unit consists of two monostable multivibrators and an amplifier identical to the one in the master generator. The first multivibrator is triggered by a signal from the master "divide-by-two" and acts as a quarter-cycle time delay. At the end of a quarter-cycle, the second multivibrator is triggered, and its output is amplified

**Figure 12-17** Phasing programmer.



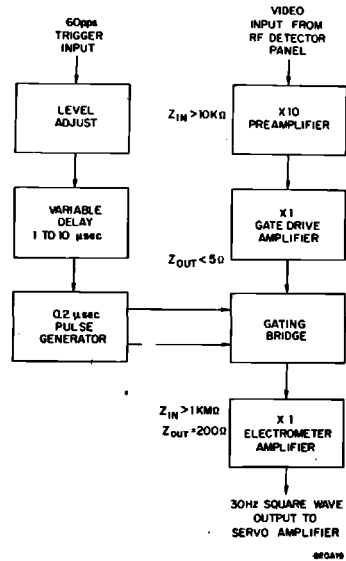


Figure 12-18 Block diagram of gated voltmeter.

to give a 30-Hz square wave in quadrature with the master generator. This waveform is applied to the reference winding of the two-phase motors which turn the phase shifters.

**THE GATED VOLTMETER.** A block diagram of this circuit is shown in Fig. 12-18. The video output from the RF detector panel is amplified in a  $\times 10$  preamplifier and fed into a sample-and-hold circuit, where a gating bridge takes a 0.2- $\mu$ sec sample, 0.5  $\mu$ sec after the beginning of the video pulse. The time constant of the sampling circuit is 40  $\mu$ sec, so that the hold circuit voltage (with a time constant of 10 sec) rises to over 95% of the sampled video voltage. The gate occurs after the appropriate trigger, selected by the programmer. The delay is adjustable so that it may be properly positioned in the video pulse. The sampled voltage is held essentially constant until the next sample is taken, so that a 30-Hz square wave is formed. As has been shown, its amplitude is proportional to the cosine of the phase across the hybrid ring.

**THE SERVO AMPLIFIER.** This amplifier increases the output of the gated voltmeter to a level which will drive the control winding of the two-phase motor. Its gain is adjusted to saturate at 20 V corresponding to a phase error of  $30^\circ$ .

**THE NULL DETECTOR.** This device is a voltage-doubling rectifier driving a back-biased saturating dc amplifier. When the servo amplifier output is

greater than 4 V peak-to-peak, the voltage out of the doubler exceeds the back-bias and a relay in the programmer is pulled in.

**THE VIDEO AMPLIFIER AND BEAM CURRENT INTERLOCK.** The amplifier, which is identical to the gated voltmeter preamplifier, boosts the level of the video output from the RF detector panel and feeds it to the video transmission system to CCR.

A beam current interlock operates from the video output of one of the coaxial thermionic diodes in the RF detector panel. The video pulse is superimposed upon a multivibrator pulse (timed by the "accelerate" trigger). If the video pulse amplitude exceeds a preset level (corresponding to 1-mA beam current), the combined voltages lift a tunnel diode and transistor amplifier circuit into conduction. The multivibrator pulse ends after 20  $\mu$ sec, biasing the tunnel diodes off and resetting the circuit. It should be noted that this circuit conducts only if a video pulse of sufficient amplitude arrives in coincidence with a multivibrator pulse. Thus, if there is no beam in the first time-slot (using for phasing), the circuit will not conduct. When there is an adequate beam, successive current pulses close a relay which enables the phasing program to proceed. Time constants are chosen so that the relay will not close if the beam repetition rate is a less than 60 pulses/sec.

## 12-6 Operational procedures (HAH, ARW)

### *Central Control Room operation*

Phasing is initiated by selecting the required sector on a switched sector panel, after having checked that the beam current through the sector in Time Slot 1 is not less than 1 mA, 1.6  $\mu$ sec pulse width, and 60 pulses/sec, and by pressing the "phase" button and the "start" button.

If required, the RF detector panel video output may be viewed by operating the video selector, although phasing is frequently initiated in many sectors in quick succession without video monitoring. However, when it is examined, the video display is very useful in diagnosing faults, as is shown in Table 12-1.

By pressing the "don't phase" button before pressing the "start" button, the programmer is made to step through without setting klystrons to standby or phasing them. This feature enables the operator at the maintenance console to examine the amplitude and phase stability of any klystron without disturbing machine operation. The "stop-start" buttons hold the programmer at any step for prolonged examination.

Appropriate use of these buttons and the "phase-don't phase" buttons permits the phase of one klystron to be adjusted without disturbing its neighbors.

As previously explained, the "fault override" button causes the programmer to proceed to the next step.

**Table 12-1 Video display and diagnosis of faults**

<i>Video indication</i>	<i>Possible cause</i>
No wobbled pattern (refer to Fig. 12-12)	<ol style="list-style-type: none"> <li>1. No cw Reference available to phasing system—varactor multiplier off or disconnected.</li> <li>2. Fault in wobbler or master generator.</li> <li>3. Klystron already phased (no fault).</li> </ol>
Wobbled pattern does not close, or "phase not OK" light stays on.	<ol style="list-style-type: none"> <li>1. Trigger or gate mistimed.</li> <li>2. Gated voltmeter or servo amplifier gain too low.</li> <li>3. Phase shifter sticking (or brake not releasing).</li> <li>4. Thermionic diode unbalance greater than 1.5 V (indicated by a large unsymmetrical "pedestal" on the klystron pulse).</li> <li>5. Rapid phase jitter on beam or klystron pulse (can be seen on video pattern).</li> </ol>

### *Operation in the sector alcove*

All the above operations can be carried out from the sector alcove by manipulating the "start" and "fault override" buttons on the programmer. However, to monitor klystrons and diode balance, it is only necessary to rotate the selector switch on the front of the RF detector panel, and the programmer is more easily controlled by using the "advance" and "klystron selector" switches.

As previously mentioned, phase shifters may also be rotated manually from the programmer.

## **12-7 Operational results (HAH, ARW)**

Correct operation of the automatic phasing system is essential to the rapid tuneup and spectrum optimization of the long accelerator.

Since the days of the first beam tests in Sector 1, it has always been possible to phase a sector locally (from the alcove) with speed (less than 1 min) and confidence (by monitoring the video on an oscilloscope), with residual phase error spread of less than  $\pm 3^\circ$ . However, random recurrence of many faults (mostly included in Table 12-1) over the full thirty sectors of the machine led to initially unreliable performance when phasing was done from CCR with no video display available there.

Experience has led to the diagnosis and elimination of recurrent faults in the programmers and electronics panels, such as programmers skipping steps because of switching transients from the phase-shifter motors, noise on the video input to the gated voltmeters, and servo loop instability due to cross-over distortion in the gated voltmeters.

With the installation of the video readout in CCR and beam current interlock, most malfunctions due to improper operating conditions have been eliminated.

Thermionic diode unbalance in the RF detector panel has always been a weakness in the reliability of the system. The trouble stems from the fact that the diode characteristics change with signal level and with time. While the wobbled signal amplitude stays within acceptable limits, as discussed earlier, divergence of the two diode characteristics at high signal levels (as produced by the klystrons) can easily result in a dc offset to the wobbled pulse which saturates the gated voltmeter preamplifier.

The present solution is to rebalance each diode pair once a week. However, for testing purposes, a "switched attenuator" has been added to the RF detector panels in two sectors. This device adds 20-dB attenuation to the RF path when the klystron is being phased and substitutes a low-attenuation, trombone phase shifter when the reference signal is being phased to the beam. The two paths are brought to the same electrical length by a fixed adjustment of the trombone. The switched attenuator certainly solved the diode unbalance problem but has the disadvantage that it could introduce an inherent phase error if the fixed length of either of the two paths should drift. Other solutions are still being sought.

In conclusion, it may be stated that the automatic phasing system is now recognized at SLAC to be an invaluable tool in the routine phase optimization of the machine, in setting up special phase conditions for positron acceleration, and for diagnosing klystron faults and intrasector beam loss.

#### *Acknowledgments*

Many people contributed to the conceptual and technical development of the automatic phasing system. The authors are particularly indebted to R. B. Neal, D. J. Goerz, and W. J. Gallagher for their contributions in formulating the idea of beam-induction phasing and to C. B. Williams and J. Dobson for much of the initial planning of the system. G. Jackson, Jr., J. R. Bordenave, P. V. Lee, K. E. Holladay, and C. E. Bolden were responsible for much of the work involved in designing, procuring, and testing system equipment.

#### **References**

- 1 D. J. Goerz and R. B. Neal, "Method of Phasing a Long Linear Electron Accelerator," Rept. No. ML-550, Microwave Laboratory, Stanford University, Stanford, California (October 1958).
- 2 W. J. Gallagher, D. Goerz, G. Loew, K. Mallory, R. Neal, and J. Pine, "Methods for Phasing Long Linear Accelerators," Rept. No. M-101, Stanford Linear Accelerator Center, Stanford University, Stanford, California (November 1958).
- 3 W. J. Gallagher, D. Goerz, G. Loew, K. Mallory, R. Neal, and J. Pine, "Methods of Driving Long Linear Accelerators," Rept. No. M-102, Stanford Linear Accelerator Center, Stanford University, Stanford, California (December 1958).

- 4 D. J. Goerz and R. B. Neal, "Phasing a Linear Accelerator from RF Phase Shift Due to Beam Loading Interaction," Rept. No. M-103, Stanford Linear Accelerator Center, Stanford University, Stanford, California (December 1958).
- 5 W. J. Gallagher, D. Goerz, G. Loew, K. Mallory, R. Neal, and J. Pine, "Comparison of Methods of Phasing Long Linear Accelerators," Rept. No. M-104, Stanford Linear Accelerator Center, Stanford University, Stanford, California (December 1958).
- 6 R. Belbéoch and C. B. Williams, "Current Variation Detection Technique of Phasing Linear Electron Accelerators," SLAC-TN-62-75, Stanford Linear Accelerator Center, Stanford University, Stanford, California (November 1962).
- 7 G. A. Loew, "Phasing System," Section III.E of the SLAC Source Book, Stanford Linear Accelerator Center, Stanford University, Stanford, California (March 1963).
- 8 K. L. Brown, A. L. Eldredge, R. H. Helm, J. H. Jasberg, J. V. Lebacqz, G. A. Loew, R. F. Mozley, R. B. Neal, W. K. H. Panofsky, and T. F. Turner, "Linear Electron Accelerator Progress at Stanford University," *Proc. Intern. Conf. High Energy Accelerators, Brookhaven, September 1961*, p. 101, U.S. Govt. Printing Office, Washington, D.C.
- 9 R. B. Neal, "Transient Beam Loading in Linear Electron Accelerators," Rept. No. ML-388, Microwave Laboratory, Stanford University, Stanford, California (May 1957).
- 10 G. A. Loew, "Non-synchronous Beam Loading in Linear Electron Accelerators," Rept. No. ML-740, Microwave Laboratory, Stanford University, Stanford, California (August 1960).
- 11 G. A. Loew, "Beam Induced Power in a Constant Gradient Accelerator Section," Tech. Note No. TN-63-19, Stanford Linear Accelerator Center, Stanford University, Stanford, California (March 1963).
- 12 A. G. Fox, "An Adjustable Waveguide Phase Changer," *Proc. Inst. Radio Engrs.* 35, 1489 (1947).
- 13 J. Dobson and M. Lee, "The Beam Induction Technique of Phasing Linear Electron Accelerators over Large Ranges of Beam Current," Tech. Note No. TN-63-70, Stanford Linear Accelerator Center, Stanford University, Stanford, California (1963).

